https://doi.org/10.1595/205651323X16902884637568 *Johnson Matthey Technol. Rev.*, 2024, **68**, (1), 49–59

JOHNSON MATTHEY
TECHNOLOGY REVIEW

technology.matthey.com

Influence of Temperature and Orientation on Elastic, Mechanical, Thermophysical and Ultrasonic Properties of Platinum Group Metal Carbides

Values at 0 K and 300 K are reported

Anurag Singh* and Devraj Singh
Department of Physics, Prof. Rajendra Singh (Rajju Bhaiya) Institute of Physical Sciences for Study and Research, Veer Bahadur Singh Purvanchal University, Jaunpur–222003, U.P., India

***Email:** anuragrajpoot440@gmail.com

PEER REVIEWED

Received 20th June 2023; Revised 23rd July 2023; Accepted 25th July 2023; Online 25th July 2023

The elastic, mechanical, thermophysical and ultrasonic properties of platinum group metal (pgm) carbides XC (X = rhodium, palladium, iridium) have been investigated at room temperature. The Coulomb and Born-Mayer potential model was used to compute second- and third-order elastic constants (SOECs and TOECs) at 0 K and 300 K. The obtained values of SOECs were used to evaluate mechanical properties such as Young's modulus, bulk modulus, shear modulus, Pugh's indicator, Zener anisotropic constant and Poisson's ratio at room temperature. The materials show brittle nature as the value of Pugh's indicator for pgm carbides is ≤1.75. The values of SOECs were used to compute the ultrasonic velocities along <100>, <110> and <111> directions for the longitudinal and shear modes of wave propagation. Further, the values of Debye temperature, thermal conductivity, specific heat per unit volume, energy density, average value of ultrasonic Grüneisen parameter, thermal relaxation time and non-linear parameter were calculated with the help of SOECs, TOECs, ultrasonic velocities, density and molecular weight. Finally, the ultrasonic attenuation due to phonon-phonon interaction and due to thermoelastic relaxation mechanisms were calculated with the use of all associated parameters. The calculated values of elastic, mechanical, thermophysical and ultrasonic properties are compared with available literature and discussed.

1. Introduction

During the past few years, much attention has been given to the study of different properties of pgms and their alloys, especially the carbides, due to their applications in science and engineering (1–5). The pgm carbides have excellent mechanical and thermophysical properties such as hardness, strength, wear resistance and high melting point. Many theoretical and experimental studies have been carried out on the structural, mechanical, dynamical, electronic and optical properties of the pgm carbides (6–14). Li *et al*. synthesised platinum carbide under extreme conditions and considered it a potential candidate for super hard materials (1). Ono *et al*. reported the synthesis of platinum carbide by the synchrotron X-ray diffraction method at pressure greater than 75 GPa at high temperature (2). Jyoti *et al*. presented a comprehensive study of elastic, mechanical, thermophysical and ultrasonic properties of novel platinum carbides in rock-salt and wurtzite structural phases at room temperature (3). Iridium carbides

with various stoichiometries were investigated by Li *et al*. using the first principles method (4). Rabah *et al*. investigated the stabilities and mechanical properties of ideal stoichiometric palladium monocarbides in five different phases (5). A study of the cohesive energies of 4*d*-transition metal carbides was performed by Guillermet *et al*. (6). Bugaev *et al*. focused on the formation of carbide phase in the bulk region and on the surface of supported palladium nanoparticles (7). They also used X-ray absorption spectroscopy to study carbide formation. The structural, electronic, vibrational and thermodynamical properties of transition metal carbides ruthenium carbide, rhodium carbide, palladium carbide and silver carbide were investigated by Soni *et al*. using the plane wave pseudopotentials method with the generalised gradient approximation (GGA) in the frame of density functional theory (8). Ateser *et al*. studied structural, mechanical and dynamic properties of palladium carbide to predict the most stable structure using a GGA approximation based on Perdew-Burke-Ernharf function synthesis (9). Properties and simulation of pgm carbides were studied by Ivanovski (10). The first principles computation method was performed to understand the peculiarities of mechanical stability, elastic and electronic properties and chemical bonding for rhodium carbide, palladium carbide and iridium carbide by Bannikov *et al*. (11). Li investigated the structural and electronic properties of palladium carbide using local density approximation and GGA (12). Tan *et al*. studied potential energy curves and spectroscopic constants of 23 states of rhodium carbide using complete active space multi configuration self-consistent field followed by first order configuration interaction calculation (13). A new method to synthesise rhodium carbide was presented by Wakisaka *et al*. (14). Ksouri *et al*. investigated structural, elastic and thermodynamic properties of metal carbides MC (M = iridium, rhodium and ruthenium) (15). Spectroscopic characterisation of chain-to-ring structural evolution in platinum carbide clusters was studied by Zhang *et al*. (16).

In view of these circumstances and taking into account that there is no precise and complete analysis available from elastic properties to ultrasonic properties of pgm carbides, we have investigated temperature dependent elastic, mechanical, thermodynamical and ultrasonic properties of pgm carbides XC (X: rhodium, palladium and iridium) along <100>, <110>, <111> crystallographic directions.

The layout of this paper is as follows: the theoretical background in Section 2; the results are presented and discussed in Section 3; Section 4 includes the concluding remarks of the investigation.

2. Theoretical Background

The Coulomb and Born-Mayer potentials were applied to compute the SOECs and TOECs for the pgm carbides at temperatures 0 K and 300 K. The theoretical calculation of elastic constants is based upon the stress-strain method expressed by Hooke's law (17). Hooke's law for an anisotropic medium can be given as:

$$\sigma_{ij} = C_{ijkl}\eta_{kl} \quad \text{(i)}$$

where i, j, k, l = 1, 2, 3 and C_{ijkl} is a fourth rank tensor called elastic stiffness constant; σ_{ij} is second rank stress tensor for the anisotropic material; and η_{kl} is the Lagrangian strain tensor:

$$\partial\eta_{kl} = \frac{1}{2}\left[\left(\frac{\partial x_k}{\partial a_1}\right)\left(\frac{\partial x_l}{\partial a_K}\right) - \delta_{ij}\right] \quad \text{(ii)}$$

where a and x are initial and final position of a material point and δ_{ij} is the Kronecker's delta.

To deform any solid elastically, work is stored in the form of potential energy. The elastic energy density is defined as the energy per unit volume of a cubic structure. The elastic energy density for a deformed solid can be expanded as a power series of strains. The coefficients of terms higher than quadratic in strains are defined as higher-order elastic constants. The elastic constant of nth order defined by (17) is:

$$C_{ijklmn} = \left(\frac{\partial^n F}{\partial\eta_{ij}\partial\eta_{ij}\partial\eta_{ij}\cdots}\right)_{\eta=0} \quad \text{(iii)}$$

The tensor notation can be written as:

$$C_{IJK\cdots} = C_{ijklmn\cdots} = \left(\frac{\partial^n F}{\partial\eta_{ij}\partial\eta_{ij}\partial\eta_{ij}\cdots}\right)_{\eta=0} \quad \text{(iv)}$$

The indices are contracted as $ij = I$, $jk = J$, 11→1, 22→2, 33→3, 23→4, 31→5, 12→6. Here, F is the free energy density of the undeformed material.

The free energy density of the material at temperature T is given as:

$$F^{Total} = U + F^{Vib} \quad \text{(v)}$$

where U stands for internal energy per unit volume of the crystal when all ions are at rest on their lattice point, which is given by:

$$U = \frac{1}{2V_C}\sum\phi_{\mu\omega}(r) \quad \text{(vi)}$$

where r is the distance between the μ^{th} and v^{th} ions; $\varphi_{\mu v}(r)$ is the interaction potential between μ^{th} and v^{th} ions. It is the sum of long-range Coulomb potential $\varphi_{\mu v}(C)$ and the short-range Born Mayer repulsive potential $\varphi_{\mu v}(B)$. V_C is the volume of the elementary cell. The interaction potential $\varphi_{\mu v}(r)$ can be expressed as:

$$\phi_{\mu v}(r) = \phi_{\mu v}(C) + \phi_{\mu v}(B) \quad \text{(vii)}$$

$\varphi(C)$ and $\varphi(B)$ may be expressed as:

$$\phi_{\mu v}(C) = \pm\left(\frac{e^2}{r_0}\right) \text{ and } \phi_{\mu v}(B) = A_{\exp}\left(-\frac{r_0}{b}\right) \quad \text{(viii)}$$

$\pm$ sign is used for like and unlike ions. Here, e is the electronic charge; r_0 is the nearest neighbour distance; A is strength parameter; and b is hardness parameter, respectively.

Strength parameter A is defined as:

$$A = -3b\left(\frac{e^2}{r_0^2}\right)(-0.5825)\left[\begin{matrix}6\exp\left(\frac{-r_0}{b}\right)\\ +12\sqrt{2}\exp\left(\frac{-\sqrt{2}r_0}{b}\right)\end{matrix}\right]^{-1} \quad \text{(ix)}$$

Vibrational free energy F^{Vib} is given by:

$$F^{Vib} = \frac{k_B T}{nV_C}\sum_{i=0}^{3sN}\ln 2\sinh(h\omega_i/2k_B T) \quad \text{(x)}$$

where n is the number of the cells in the crystal; s is the number of ions per unit cell; ω_i is vibrational frequency corresponding to i^{th} mode of atomic vibration; and k_B is the Boltzmann constant.

Elastic constants of second and third order at temperature T from Equations (iv), (v) and (vi) are written as:

$$C_{IJ} = C_{IJ}^0 + C_{IJ}^{Vib} \text{ and } C_{IJK} = C_{IJK}^0 + C_{IJK}^{Vib} \quad \text{(xi)}$$

The SOECs and TOECs are obtained as the sum of static elastic constants at absolute zero temperature and vibrational energy contribution at a particular temperature; the superscript 0 indicates the static constant at 0 K and superscript 'vib' indicates the vibrational portion of elastic constant at a certain temperature. The expressions to compute SOECs and TOECs are given in the literature (18).

The SOECs are applied to compute the mechanical properties of pgm carbides such as bulk modulus (B), shear modulus (G), Young's modulus (Y), Poisson's ratio (σ), Zener anisotropy (A_n) and Pugh's ratio (B/G) at room temperature (17, 18). The expressions for B, Y, G, σ and A_n are:

$$B = \frac{(C_{11} + 2C_{12})}{3} \quad \text{(xii)}$$

$$G = \frac{(C_{11} - C_{12} + 3C_{44})}{10} + \frac{2.5(C_{11} - C_{12})C_{44}}{(4C_{44} + 3(C_{11} - C_{12})} \quad \text{(xiii)}$$

$$Y = \frac{9GB}{(G + 3B)} \quad \text{(xiv)}$$

$$\sigma = \frac{(3B - 2G)}{(6B + 2G)} \quad \text{(xv)}$$

$$A_n = \frac{2C_{44}}{(C_{11} - C_{12})} \quad \text{(xvi)}$$

Further SOECs of pgm carbides were used to compute the ultrasonic velocities along different directions. When an acoustic wave propagates through pgm carbides, it diffuses into one longitudinal and two shear acoustic waves. There are three modes of acoustic velocity: V_L, V_{S1} and V_{S2} along <100>, <110> and <111> crystallographic directions. The acoustic velocity depends on SOECs and mass density in the following ways:

along <100> direction:

$$V_L = \sqrt{(C_{11}/\rho)}; \quad V_{S1} = V_{S2} = \sqrt{(C_{44}/\rho)}; \quad \text{(xvii)}$$

along <111> direction:

$$V_L = \sqrt{(C_{11} + 2C_{12} + 4C_{44})/3\rho};$$
$$V_{S1} = V_{S2} = \sqrt{(C_{11} - C_{12} + C_{44})/3\rho}; \quad \text{(xviii)}$$

along <110> direction:

$$V_L = \sqrt{(C_{11} + C_{12} + 2C_{44})/2\rho};$$
$$V_{S1} = \sqrt{C_{44}/\rho};\ V_{S2} = \sqrt{(C_{11} - C_{12})/\rho}; \quad \text{(xix)}$$

From ultrasonic velocities the Debye average velocity (V_D) can be calculated in the following way:

along <100> and <111> direction

$$V_D = \left[\frac{1}{3}\left\{\frac{1}{V_L^3} + \frac{2}{V_{S1}^3}\right\}\right]^{-1/3} \quad \text{(xx)}$$

along <110> direction

$$V_D = \left[\frac{1}{3}\left\{\frac{1}{V_L^3} + \frac{1}{V_{S1}^3} + \frac{1}{V_{S2}^3}\right\}\right]^{-1/3} \quad \text{(xxi)}$$

The Debye average velocity is used to calculate the Debye temperature (θ_D) (17) as follows:

$$\theta_D = \frac{h}{k_B}\left(\frac{3nN\rho}{4\pi M}\right)^{1/3} V_D \quad \text{(xxii)}$$

where k_B is Boltzmann's constant; N is Avogadro's number; h is Planck's constant; M is the molecular weight; ρ is the density; and n is number of atoms per unit cell. The Debye temperature is used to compute the thermal conductivity (κ). The expression for κ is:

$$\kappa = \frac{A\bar{M}_a\delta\theta_D^3\, n^{1/3}}{\gamma^2 T} \quad \text{(xxiii)}$$

where δ (in Å) is the cube root of volume per atom; $A = 3.04 \times 10^{-8}$; $\bar{M}_a$ is defined as average atomic mass in amu; γ is defined as the Grüneisen parameter. Grüneisen parameter along different directions was computed using SOECs and TOECs (19). κ is defined as thermal conductivity which was calculated by Morelli and Slack's approach (20). When ultrasonic waves pass through pgm carbides, the energy is dissipated. The loss in the material occurs for different reasons, for example electron-phonon interaction, phonon-phonon interaction, thermoelastic relaxation, grain boundaries and magnon-phonon interaction. At temperature ≥100 K the most conspicuous causes of ultrasonic losses in the pgm carbides are Akhieser loss (phonon-phonon interaction) and loss due to thermal relaxation mechanisms. The computation of ultrasonic attenuation in the chosen pgm carbides was done using Mason's approach (19). The ultrasonic attenuation due to Akhieser loss is given by:

$$\left(\frac{\alpha}{\nu^2}\right)_L = \frac{4\pi^2\tau_L E_0 D_L}{6\rho V_L^3} \quad \text{(xxiv)}$$

$$\left(\frac{\alpha}{\nu^2}\right)_{S1} = \frac{4\pi^2\tau_{S1} E_0 D_{S1}}{6\rho V_{S1}^3} \quad \text{(xxv)}$$

$$\left(\frac{\alpha}{\nu^2}\right)_{S2} = \frac{4\pi^2\tau_{S2} E_0 D_{S2}}{6\rho V_{S2}^3} \quad \text{(xxvi)}$$

where α is the ultrasonic attenuation constant; ν is the frequency of ultrasonic wave; V_L is the ultrasonic velocity for longitudinal wave; E_0 energy density which is computed by (θ_D/T) (21). The required time in which thermal phonons regain their original shape distorted by ultrasonic waves for exchange of acoustic and thermal energy is known as thermal relaxation time (τ_{th}) and is given as:

$$\tau_{th} = \tau_S = \frac{\tau_L}{2} = \frac{3\kappa}{C_V V_D^2} \quad \text{(xxvii)}$$

where C_V is specific heat capacity at constant volume computed using data from the AIP handbook (21); D is non-linearity parameter (acoustic coupling constant) given by:

$$D = 9 <(\gamma_i^j)^2> - \frac{3(<\gamma_i^j>)^2 C_V T}{E_0} \quad \text{(xxviii)}$$

The thermoelastic attenuation caused by thermoelastic relaxation is given by (21):

$$\left(\frac{\alpha}{\nu^2}\right)_{th} = \frac{4\pi^2\langle\gamma_i^j\rangle^2\,\kappa T}{2\rho V_L^5} \quad \text{(xxix)}$$

3. Results and Discussion

The computed values of SOECs and TOECs for the chosen pgm carbides were obtained using Coulomb and Born-Mayer potential model. The two parameters, nearest neighbour distance and hardness parameter, play important roles in evaluating SOECs and TOECs for the pgm carbides. The nearest neighbour distance (r_0) for rhodium carbide, palladium carbide and iridium carbide are 2.172 Å, 2.215 Å and 2.20 Å respectively (11). These values are assumed to be constant at temperatures 0 K and 300 K and hardness parameter b is selected 0.303 Å for all materials (22).

The computed values of SOECs and TOECs using Equations (i)–(xi) for the pgm carbides are presented in **Table I** at 0 K and 300 K with existing comparable SOECs (3, 9, 11, 23–26). There are some variations in the obtained results and existing results as we have neglected the polarisability of the ions, van der Waal's forces and many body forces. It is obvious from **Table I** that values of elastic constants are highest for rhodium carbide and lowest for palladium carbide, which shows that rhodium carbide has better intrinsic properties among the chosen pgm carbides. **Table I** depicts that the values of C_{11} and C_{44} increase while C_{12} decreases with increase in temperature for the chosen materials. The TOECs C_{111}, C_{112}, C_{116} are negative and decrease with increase in temperature; C_{123} decreases with temperature while C_{144} increases with temperature and the value of C_{456} remains constant due to absence of vibrational energy. C_{11}, C_{12}, C_{44}, C_{123}, C_{144} have positive temperature coefficients and C_{111}, C_{112}, C_{166} have negative temperature coefficients while C_{456} remains constant irrespective of temperature change. Because there is no contribution of vibrational energy, Cauchy's relations defined by Cousin at 0 K are satisfied: $C_{12}^0 = C_{44}^0$; $C_{112}^0 = C_{166}^0$; $C_{123}^0 = C_{456}^0 = C_{144}^0$ in present case (27). Cauchy's relation holds good at 0 K but does not hold good at higher temperatures because on increasing temperature the nature of the interacting forces becomes more ionic. The orders of the elastic constants of the investigated materials are comparable with platinum carbide (3). The SOECs obeyed the Born stability criterion ($C_{11}+2C_{12} > 0$, $C_{44} > 0$, $C_{11}-C_{12} > 0$) which proves that the chosen materials are elastically stable at room temperature in B1 phase (28). The TOECs are higher for rhodium carbide and lower for palladium carbide. TOEC values are not available for direct comparison for pgm carbides, so the results of TOEC calculations

Table I Second-Order and Third-Order Elastic Constants of Platinum Group Metal Carbides at 0 K and 300 K

Material	Temperature, K	Elastic constants, 10^{11} Nm^{-2}								
		C_{11}	C_{12}	C_{44}	C_{111}	C_{112}	C_{123}	C_{144}	C_{166}	C_{456}
RhC	0	7.39	4.67	4.67	–106.67	–19.04	7.03	7.03	–19.04	7.03
	300	8.39	4.58	4.73	–114.46	–19.76	5.6	7.09	–19.34	7.03
		2.927[a]	1.819[a]	0.454[a]	–	–	–	–	–	–
		4.25b	2.51[b]	0.43[b]	–	–	–	–	–	–
		4.39[c]	2.56[c]	–	–	–	–	–	–	–
PdC	0	7.27	4.29	4.29	–105.85	–17.5	6.5	6.5	–17.5	6.5
	300	8.24	4.19	4.34	–113.64	–18.2	5.06	6.56	–17.79	6.5
		3.76[b]	1.73[b]	0.56[b]	–114.67[d]	–12.59[d]	4.09[d]	4.75[d]	–13.12[d]	4.67[d]
		2.76[c]	1.81[c]	0.49[d]	–	–	–	–	–	–
		3.72[d]	3.07[d]	–	–	–	–	–	–	–
Pd	300	3.21[e]	2.44[e]	1.11[e]	–	–	–	–	–	–
		1.94[f]	1.50[f]	0.72[f]	–	–	–	–	–	–
IrC	0	7.31	4.41	4.42	–106.16	–18.02	6.68	6.68	–18.02	6.68
	300	8.29	4.32	4.47	–113.9	–18.72	5.24	6.74	–18.31	6.68
		4.39[c]	2.57[c]	–	–	–	–	–	–	–
Ir	300	5.80[g]	2.42[g]	2.56[g]	–	–	–	–	–	–

[a]See (9); [b]See (11); [c]See (23); [d]See (3); [e]See (25); [f]See (26); [g]See (24)

Table II Mechanical Properties of Platinum Group Metal Carbides at Room Temperature

Material	*Y*, 10^{11} Nm^{-2}	*B*, 10^{11} Nm^{-2}	*G*, 10^{11} Nm^{-2}	*B/G*	*Σ*	A_n
RhC	8.31	5.85	3.29	1.78	0.26	2.48
	1.23[a]	2.844[b]	–	–	0.43[a]	–
	–	3.09[a]	–	–	–	–
	–	2.82[c]	–	–	–	–
Rh	3.86[d]	2.80[d]	1.53[d]	1.83[d]	0.26[d]	–
PdC	8.05	5.54	3.2	1.73	0.26	2.14
	1.56[e]	2.68[b]	0.49[a]	4.456[a]	0.396[a]	3.2[c]
	1.17[c]	2.188[a]	0.42[c]	–	0.39[e]	–
	–	2.78[f]	–	–	–	–
	–	2.41[e]	–	–	–	–
	–	2.13[c]	–	–	–	–
Pd	–	2.70[g]	–	–	–	–
	1.28[d]	1.90[d]	0.46[d]	4.13[d]	0.39[d]	–
IrC	8.14	5.64	3.23	1.75	0.26	2.25
	–	3.18[d]	–	–	–	–
Ir	5.38[d]	3.78[d]	2.14[d]	1.78[d]	0.26[d]	–

[a]See (9); [b]See (32); [c]See (23); [d]See (33); [e]See (11); [f]See (12); [g]See (25)

for the chosen pgm carbides are compared with our recent publication on platinum carbide. The order of the TOECs has the same quantum (3). SOECs of pgm carbides were found to be higher than those for pgm pure metals. These elastic constants were further applied to compute various mechanical constants like Young's modulus (Y), bulk modulus (B), shear modulus (G), Pugh's ratio (B/G), Poisson's ratio (σ) and Zener anisotropic ratio (A_n) using Equations (xii)–(xvi) and are presented in **Table II**.

From **Table II** it is clear that bulk modulus and Young's modulus for rhodium carbide are highest and those for palladium carbide are lowest which predicts that rhodium carbide is stiffer and less compressible than other pgm carbides. The higher value of shear modulus for rhodium carbide shows that it is much harder than palladium carbide and iridium carbide. The calculated Pugh's ratios for the chosen materials are ≤1.75 which shows that the chosen pgm carbides are brittle in nature (29, 30). The Poisson's ratio limit for non-central nature of interatomic forces is given by $0.2<\sigma<0.5$. In the present case, the calculated value of Poisson's ratio is 0.26 which shows that applied forces are non-central in pgm carbide materials (31). For covalent materials Poisson's ratio is almost 0.1 while it is 0.25 for an ionic bond. The calculated Poisson's ratio is greater than 0.25 which shows that ionic contributions in interatomic bonding are dominant for the chosen materials. With the help of Poisson's ratio (σ) and Cauchy pressure ($C_{12}–C_{44}$), the intrinsic ductility and brittleness can be predicted for the pgm carbides. For ductile materials, Poisson's ratio $\sigma>0.3$ and Cauchy pressure $(C_{12}–C_{44})>0$, while for brittle materials Poisson's ratio $\sigma<0.3$ and Cauchy pressure $(C_{12}–C_{44})<0$. From **Table II**, the values of Poisson's ratio for pgm carbides are less than 0.3 ($\sigma<0.3$) and Cauchy's pressure is less than zero $(C_{12}–C_{44}<0)$ for all chosen pgm carbides. This confirms the chosen pgm carbides are brittle in nature.

For isotropic materials A_n should be equal to one but in our case A_n is greater than one which indicates the chosen materials are anisotropic in nature. The obtained values are compared with existing values in available literatures (9, 11, 12, 23, 26, 32, 33). The variations in the results are due to different computational methods. Our calculations are based on MATLAB® and manual calculation which gives precise results.

To study changes in elastic, mechanical, thermophysical and ultrasonic properties exhibited by pgm carbides we have compared the properties of the pgm carbides with the known properties of pgms as shown in **Tables I** and **II**. If we compare mechanical properties of pgm carbides (rhodum carbide, palladium carbide and iridium carbide) to existing values of pure pgms (rhodium, palladium and iridium) we find that values of Young's modulus, bulk modulus and shear modulus of pgms are lower than those of pgm carbides. Pugh's ratio for pgms is >1.75 which shows the ductile nature of pgms. Thus pgms are softer and more ductile while pgm carbides are harder and brittle in nature.

The values of ultrasonic velocity for any material depends on SOECs and density along <100>, <110> and <111> directions for longitudinal and shear modes of wave propagation. The ultrasonic velocities (V_L and V_s) were computed using Equations (xvii)–(xix). The Debye average velocity V_D was computed using Equations (xx)–(xxi) along different directions. The computed values of V_L, V_S and V_D are presented in **Table III**.

The Debye average velocity is highest for rhodium carbide along <100> direction and lowest for iridium carbide along <110> direction. The calculated values are compared with the values obtained by Ateser *et al*. (9) which is in approximate agreement with the values of palladium carbide along <100> direction. The decreasing value of ultrasonic velocity from rhodium carbide to iridium carbide is due to an increase in density. The Debye temperature (θ_D) is the temperature of a crystal's highest normal mode of vibration and it correlates elastic properties with thermodynamic properties such as phonons, thermal expansion, thermal conductivity, specific heat and lattice enthalpy (32, 34). θ_D was computed using Equation (xxii). The computed values of θ_D along different directions are presented in **Figure 1**.

Figure 1 shows that the value of θ_D is lowest along <110> direction for all materials. It is also mentionable here that the value of θ_D is smallest for iridium carbide, because θ_D is proportional to the cube root of the molecular weight. The value of θ_D along <100> direction for palladium carbide is 319 K in our case while Ateser *et al*. presented θ_D 353 K. Standard values of Debye temperature for rhodium, palladium and iridium are 275 K, 150 K and 228 K respectively (9). Average Grüneisen parameter $<\gamma_i^j>$ was evaluated with the help of SOECs and TOECs. Further, θ_D and $<\gamma_i^j>$ were applied to compute thermal conductivity (κ) using Equation (xxiii). The specific heat per unit volume (C_V) and energy density (E_0) were calculated using (θ_D/T) tables (19). The computed values of $<\gamma_i^j>$, κ, C_V and E_0 are presented in **Table IV**.

Table III Orientation-Dependent Ultrasonic Velocities of Platinum Group Metal Carbides at Room Temperature

Material	Direction	Ultrasonic Velocities, 10^3 ms^{-1}			
		V_L	V_{S1}	V_{S2}	V_D
RhC	<100>	3.00	2.25	2.25	2.42
	<110>	3.47	2.25	1.43	1.88
	<111>	3.61	1.75	1.75	1.97
PdC	<100>	3.02	2.19	2.19	2.37
		5.85[a]	1.98[a]	1.98[a]	2.25[a]
	<110>	3.42	2.19	1.50	1.93
		5.60[a]	1.98[a]	2.88[a]	2.34[a]
	<111>	3.54	1.76	1.76	1.98
		5.593[b]	2.324[b]	1.75[a]	2.63[b]
		5.65[a]	1.75[a]	–	1.99[a]
Pd	<100>	4.743[c]	–	–	–
	<110>	2.436[c]			
	<111>	1.456[c]			
IrC	<110>	2.28	1.68	1.68	1.81
	<111>	2.6	1.68	1.12	1.45
	<111>	2.7	1.33	1.33	1.49

[a]See (3); [b]See (9); [c]See (35)

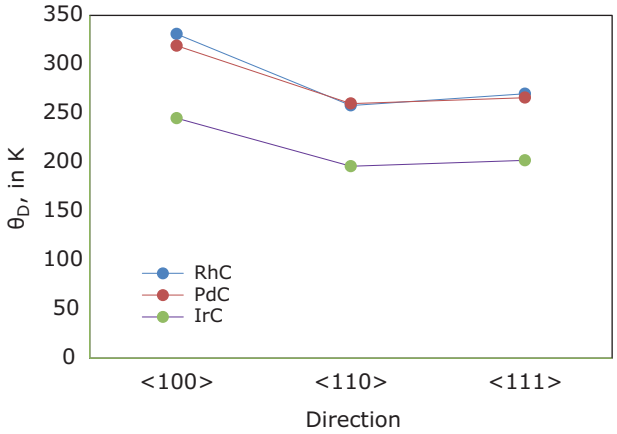

Fig. 1. Direction-dependent Debye temperature of pgm carbides

It is obvious from **Table IV** that the ultrasonic Grüneisen parameters calculated using Mason's approach are highest along <111> direction. The thermal conductivity directly depends on atomic weight and Debye temperature. It can be seen in **Table IV** that the thermal conductivity increases with increasing atomic weight and Debye temperature. The values of thermal conductivity for pgm carbides are highest along <100> direction. The value of thermal conductivity is highest for rhodium carbide and lowest for iridium carbide because the thermal conductivity is directly proportional to the Debye temperature. The existing values of κ for rhodium, palladium and iridium are 150 Wm^{-1} K^{-1}, 72 Wm^{-1} K^{-1} and 150 Wm^{-1} K^{-1} respectively which indicates that pure pgms are thermally stronger than pgm carbides. The values of specific heat capacity (C_V) and energy density (E_0) are highest for iridium carbide along <110> direction and lowest for rhodium carbide along <100> direction. The values of C_V for rhodium carbide and palladium carbide materials are approximately equal.

The thermal relaxation times (τ_{th}) were calculated using Equation (xxvii). The values of acoustic coupling constants (D_L and D_S) for longitudinal and shear waves were computed using average Grüneisen parameter $<\gamma_i^j>$ and average of the square of the Grüneisen parameter, specific heat per unit volume and energy density from Equations (xxviii)–(xxix).

All obtained thermal parameters were applied to compute the ultrasonic attenuation due to thermoelastic mechanism $(\alpha/v^2)_{th}$ and due to phonon-phonon interaction mechanism for longitudinal and shear waves $[(\alpha/v^2)_L$ and $(\alpha/v^2)_S]$ using Equations (xxiv)–(xxvi). The computed values of τ_{th}, D_L, D_S, $(\alpha/v^2)_{th}$, $(\alpha/v^2)_L$ and $(\alpha/v^2)_S$ are presented in **Table V**.

Table V shows that the value of the thermal relaxation time (τ_{th}) is of the order of 10^{-11} s which confirms the metallic character of pgm carbides (36). The value of (τ_{th}) is highest along <100> direction and lowest along <111> direction for rhodium carbide, palladium carbide and iridium carbide and it plays a crucial role in the computation of ultrasonic attenuation.

It is obvious from **Table V** that the value of acoustic coupling constant for shear wave is highest along <110> direction and polarisation along <1$\bar{1}$0> direction of the chosen B1 structured rhodium carbide, palladium carbide and iridium carbide single crystals, which indicates maximum conversion of ultrasonic energy into thermal energy

Table IV Direction-Dependent Average Grüneisen Parameter, Thermal Conductivity, Specific Heat Per Unit Volume and Energy Density for Platinum Group Metal Carbides at 300 K

Material	Direction	$<\gamma_i^j>$	κ, Wm^{-1} K^{-1}	C_V, J mole^{-1} K^{-1}	E_0, J mol^{-1}
RhC	<100>	1.38	15.29	2.356	4.856
	<110>	1.47	6.31	2.402	5.361
	<111>	1.60	6.09	2.402	5.274
PdC	<100>	1.35	14.80 9.08[a]	2.356	4.936
	<110>	1.43	7.10 9.49[a]	2.402	5.339
	<111>	1.56	6.41 8.78[a]	2.402	5.295
IrC	<100>	1.36	11.34	2.432	5.448
	<110>	1.45	5.17	2.440	5.831
	<111>	1.58	4.77	2.440	5.785

[a]See (3)

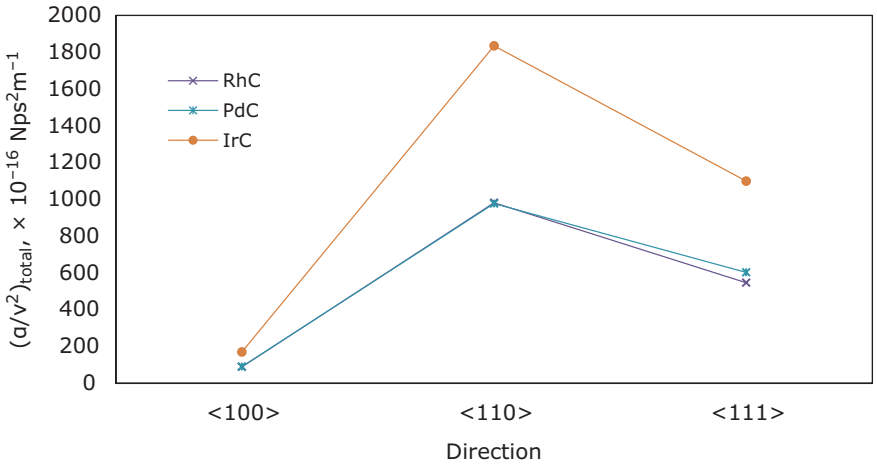

Fig. 2. Direction-dependent total ultrasonic attenuation of pgm carbides

or *vice versa*. The values of acoustic coupling constants are not available for direct comparison, therefore a comparison is made of the results of D_L and D_S with platinum carbide which shows a similar trend (3).

The ultrasonic attenuation for the chosen pgm carbides, i.e. $(\alpha/v^2)_{total} = (\alpha/v^2)_{th} + (\alpha/v^2)_L + (\alpha/v^2)_{S1} + (\alpha/v^2)_{S2}$, is shown in **Figure 2**.

From **Table V** it is clear that values of thermal attenuation loss $(\alpha/v^2)_{th}$ for XC (X = rhodium, palladium, iridium) is highest along <100> direction and lowest along <111> direction. The thermal attenuation is highest for iridium carbide which indicates that time for conversion of acoustic to thermal energy is longest for iridium carbide. From **Table V** it is also clear that thermal attenuation loss is significantly lower than loss due to phonon-phonon interaction. Computed values of Akhieser damping for the chosen materials are highest along <110> direction and lowest along <100> direction. It is also shown in **Figure 2** that total ultrasonic attenuation is highest along <110> direction at room temperature. Uncertainty in ultrasonic attenuation depends on several parameters including SOECs, TOECs, material density, heat capacity, thermal energy density, thermal relaxation time, frequency and acoustic coupling constants. Results on ultrasonic attenuation for rhodium carbide, palladium carbide and iridium carbide are not available, so comparison was done with platinum carbide (3) and good agreement was found.

Table V Direction-Dependent Thermal Relaxation Time, Acoustic Coupling Constants and Ultrasonic Attenuation of Platinum Group Metal Carbides

Material	Direction	τ_{th}, ps	Acoustic coupling constants			Ultrasonic attenuation, 10^{-16} Np s^2 m^{-1}			
			D_L	D_{S1}	D_{S2}	$(\alpha/v^2)_{th}$	$(\alpha/v^2)_L$	$(\alpha/v^2)_{S1}$	$(\alpha/v^2)_{S2}$
RhC	<100>	33.25	26.51	32.97	32.97	0.76	22.37	32.86	32.86
	<110>	22.34	26.74	44.56	324.82	0.17	10.83	32.93	937.93
	<111>	19.68	33.55	196.13	196.13	0.16	10.44	268.90	268.90
PdC	<100>	33.58	25.67	29.50	29.50	0.70	22.48	33.79	33.79
			105.50[a]	43.80[a]	–	0.58[a]	7.93[a]	34.78[a]	34.78[a]
	<110>	23.79	25.00	39.91	338.03	0.21	11.57	35.02	93.02
			78.21[a]	72.30[a]	–	0.42[a]	5.00[a]	52.25[a]	134.80[A]
	<111>	20.51	31.41	204.07	204.07	0.18	11.18	29.59	29.59
			129.50[a]	269.30[a]	–	0.31[a]	11.47[a]	40.20[a]	40.20[a]
IrC	<100>	43.00	26.51	30.60	30.60	1.26	43.19	62.90	62.90
	<110>	30.30	26.13	41.34	333.63	0.34	21.66	64.09	1748.40
	<111>	26.31	32.81	201.45	201.45	0.31	20.96	538.76	538.76

[a]See (3)

4. Concluding Remarks

In this work, the temperature- and orientation-dependent elastic, mechanical, thermal and ultrasonic properties of rock-salt structured pgm carbides were analysed. The behaviour of SOECs and TOECs were found to be like other rock-salt structured materials of B1 type. Cauchy's relation is satisfied at 0 K and the values deviate at higher temperatures for the chosen pgm carbides. The Born stability criterion for mechanical stability is satisfied by rhodium carbide, palladium carbide and iridium carbide. Pugh's ratio and Cauchy's pressure confirms the brittle nature of the investigated materials. The ultrasonic velocities are dependent on direction rather than temperature and the most suitable direction of ultrasonic wave propagation is <100> for all pgm carbides. Direction-dependent Debye temperature at which all the vibrational modes are excited is highest along <100> direction for all materials. The highest value of thermal conductivity is for rhodium carbide and lowest for iridium carbide because the thermal conductivity is directly proportional to the Debye temperature. Order of thermal relaxation time confirms the metallic nature of pgm carbides. The value of ultrasonic attenuation is lowest along <100> direction for all chosen materials, which indicates that <100> direction is most suitable for wave propagation for pgm carbides. The achieved results provide the base for further studies of these materials as well as for their engineering applications in industry.

Acknowledgement

With great pleasure, we express our sincere gratitude to the Uttar Pradesh Higher Education Council Board, Lucknow for the financial support.

References

1. Q. Li, X. Zhang, H. Liu, H. Wang, M. Zhang, Q. Li, Y. Ma, *Inorg. Chem.*, 2014, **53**, (11), 5797
2. S. Ono, T. Kikegawa, Y. Ohishi, *Solid State Commun.*, 2005, **133**, (1), 55
3. B. Jyoti, S. Triapthi, S. P. Singh, D. K. Singh, D. Singh, *Mater. Today Commun.*, 2021, **27**, 102189
4. X. Li, X. P. Du, Y. X. Wang, *J. Phys. Chem. C*, 2011, **115**, (14), 6948
5. M. Rabah, S. Benalia, D. Rached, B. Abidri, H. Rached, G. Vergoten, *Comput. Mater. Sci.*, 2010, **48**, (3), 556

6. A. F. Guillermet, J. Häglund, G. Grimvall, *Phys. Rev. B*, 1992, **45**, (20), 11557
7. A. L. Bugaev, O. A. Usoltsev, A. A. Guda, K. A. Lomachenko, I. A. Pankin, Y. V. Rusalev, H. Emerich, E. Groppo, R. Pellegrini, A. V. Soldatov, J. A. van Bokhoven, C. Lamberti, *J. Phys. Chem. C*, 2018, **122**, (22), 12029
8. H. R. Soni, S. K. Gupta, P. K. Jha, *Phys. B: Condens. Matter*, 2011, **406**, (19), 3556
9. E. Ateser, H. B. Ozisik, E. Deligoz, K. Colakoglu, *Int. J. Mod. Phys. B*, 2013, **27**, (06), 1350016
10. A. L. Ivanovskii, *Russ. Chem. Rev.*, 2009, **78**, (4), 303
11. V. V. Bannikov, I. R. Shein, A. L. Ivanovskii, *J. Phys. Chem. Solids*, 2010, **71**, (5), 803
12. L. Li, *Mod. Phys. Lett. B*, 2008, **22**, (30), 2937
13. H. Tan, M. Liao, K. Balasubramanian, *Chem. Phys. Lett.*, 1997, **280**, (5–6), 423
14. T. Wakisaka, K. Kusada, D. Wu, T. Yamamoto, T. Toriyama, S. Matsumura, H. Akiba, O. Yamamuro, K. Ikeda, T. Otomo, N. Palina, Y. Chen, L. S. R. Kumara, C. Song, O. Sakata, W. Xie, M. Koyama, Y. Kubota, S. Kawaguchi, R. L. Arevalo, S. M. Aspera, E. F. Arguelles, H. Nakanishi, H. Kitagawa, *J. Am. Chem. Soc.*, 2019, **142**, (3), 1247
15. R. Ksouri, R. Maizi, A.-G. Boudjahem, I. Djaghout, M. Derdare, R. Merdes, *Phys. Met. Metallogr.*, 2022, **123**, (13), 1376
16. Y. Zhang, S. Du, Z. Zhao, H. Han, G. Li, J. Zou, H. Xie, L. Jiang, *J. Energy Chem.*, 2023, **77**, 529
17. J. Bala, D. Singh, *Eng. Appl. Sci. Res.*, 2020, **47**, (2), 182
18. J. Bala, S. P. Singh, A. K. Verma, D. K. Singh and D. Singh, *Indian J. Phys.*, 2022, **96**, (11), 3191
19. W. P. Mason, 'Effect of Impurities and Phonon Processes on the Ultrasonic Attenuation of Germanium, Crystal Quartz, and Silicon', in "Physical Acoustics", ed. W. P. Mason, ch. 6, Vol. 3, Part B, Academic Press Inc, New York, USA, 1965, pp. 235–286
20. D. T. Morelli, G. A. Slack, 'High Lattice Thermal Conductivity Solids', in "High Thermal Conductivity Materials", eds. S. L. Shindé, J. S. Goela, ch. 2, Springer Science and Business Media Inc, New York, USA, 2006, pp. 37–68
21. "American Institute of Physics Handbook", ed. D. E. Gray, 3rd Edn., McGraw-Hill Inc, New York, USA, 1972
22. M. P. Tosi, 'Cohesion of Ionic Solids in the Born Model', in "Solid State Physics: Advances in Research and Applications", eds. F. Seitz, D. Turnbull, Vol. 16, Academic Press Inc, New York, USA, 1964, pp. 1–120
23. N. I. Medvedeva, A. L. Ivanovskii, *Phys. Status Solidi*, 2014, **251**, (1), 148
24. R. E. MacFarlane, J. A. Rayne, C. K. Jones, *Phys. Lett.*, 1966, **20**, (3), 234
25. C. V. Pandya, P. R. Vyas, T. C. Pandya, N. Rani, V. B. Gohel, *Phys. B: Condens. Matter*, 2001, **307**, (1–4), 138
26. Y. J. Sun, K. Xiong, S. M. Zhang, Y. Mao, *Mater. Sci. Forum*, 2019, **944**, 761
27. C. S. G. Cousins, *J. Phys. C: Solid State Phys.*, 1971, **4**, (10), 1117
28. M. Born, K. Huang, M. Lax, *Am. J. Phys.*, 1955, **23**, (7), 474
29. S. F. Pugh, *London, Edinburgh, Dublin Philos. Mag. J. Sci.*, 1954, **45**, (367), 823
30. D. G. Pettifor, *Mater. Sci. Technol.*, 1992, **8**, (4), 345
31. J. P. Watt, L. Peselnick, *J. Appl. Phys.*, 1980, **51**, (3), 1525
32. X. Luo, B. Wang, *J. Appl. Phys.*, 2008, **104**, (7), 073518
33. A. S. Darling, *Platinum Metals Rev*. 1966, **10**, (1), 14
34. C. Li, Z. Wang, 'Computational Modelling and *ab initio* Calculations in MAX Phases – I', in "Advances in Science and Technology of $M_{n+1}AX_n$ Phases", Woodhead Publishing Ltd, Sawston, UK, 2012, pp. 197–222
35. D. K. Hsu, R. G. Leisure, *Phys. Rev. B*, 1979, **20**, (4), 1339
36. D. Singh, D. K. Pandey, P. K. Yadawa, *Cent. Eur. J. Phys.*, 2009, **7**, (1), 198

The Authors

Anurag Singh is pursuing a PhD in Advanced Materials under supervision of Professor Devraj Singh at the Department of Physics, Prof. Rajendra Singh (Rajju Bhaiya) Institute of Physical Sciences for Study and Research, Veer Bahadur Singh Purvanchal University, Jaunpur, India. His research interests are in elastic, mechanical, thermophysical and ultrasonic properties of advanced materials.

Devraj Singh is Professor in the Department of Physics, Prof. Rajendra Singh (Rajju Bhaiya) Institute of Physical Sciences for Study and Research, Veer Bahadur Singh Purvanchal University, Jaunpur, India. He completed his DPhil in Science from the University of Allahabad, India. His research and area of study include the mechanical, thermophysical and ultrasonic properties of condensed materials. He is a life fellow of the Ultrasonics Society of India and Acoustical Society of India, life member of Materials Research Society of India, Metrology Society of India, Indian Association of Physics Teachers, Indian Physics Association and Ion Beam Society of India. He has more than 116 research articles published in national and international journals and 24 books to his credit.